THE PROTEIN SOCIETY

Structure of human peptidyl-prolyl *cis–trans* isomerase FKBP22 containing two EF-hand motifs

Sergei P. Boudko,[1,2] Yoshihiro Ishikawa,[1,2] Jay Nix,[3] Michael S. Chapman,[2] and Hans Peter Bächinger[1,2]*

[1]Research Department, Shriners Hospital for Children, Portland, Oregon 97239

[2]Department of Biochemistry and Molecular Biology, Oregon Health and Science University, Portland, Oregon 97239

[3]Molecular Biology Consortium, Advanced Light Source Beamline, Lawrence Berkeley National Laboratory, Berkeley, California 94720

Received 18 September 2013; Revised 23 October 2013; Accepted 24 October 2013
DOI: 10.1002/pro.2391
Published online 29 October 2013 proteinscience.org

Abstract: The FK506-binding protein (FKBP) family consists of proteins with a variety of protein–protein interaction domains and versatile cellular functions. It is assumed that all members are peptidyl-prolyl *cis–trans* isomerases with the enzymatic function attributed to the FKBP domain. Six members of this family localize to the mammalian endoplasmic reticulum (ER). Four of them, FKBP22 (encoded by the *FKBP14* gene), FKBP23 (*FKBP7*), FKBP60 (*FKBP9*), and FKBP65 (*FKBP10*), are unique among all FKBPs as they contain the EF-hand motifs. Little is known about the biological roles of these proteins, but emerging genetics studies are attracting great interest to the ER resident FKBPs, as mutations in genes encoding *FKBP10* and *FKBP14* were shown to cause a variety of matrix disorders. Although the structural organization of the FKBP-type domain as well as of the EF-hand motif has been known for a while, it is difficult to conclude how these structures are combined and how it affects the protein functionality. We have determined a unique 1.9 Å resolution crystal structure for human FKBP22, which can serve as a prototype for other EF hand-containing FKBPs. The EF-hand motifs of two FKBP22 molecules form a dimeric complex with an elongated and predominantly hydrophobic cavity that can potentially be occupied by an aliphatic ligand. The FKBP-type domains are separated by a cleft and their putative active sites can catalyze isomerazation of two bonds within a polypeptide chain in extended conformation. These structural results are of prime interest for understanding biological functions of ER resident FKBPs containing EF-hand motifs.

Keywords: FKBP22; *FKBP14*; EF-hand motif; Ehlers–Danlos syndrome; peptidyl-prolyl *cis–trans* isomerase; crystal structure

Introduction

Two protein families, the FK506-binding proteins (FKBPs) and the cyclosporin A-binding cyclophilins, are named for their ability to bind immunosuppressive drugs. These proteins are peptidyl-prolyl isomerases (PPIases) that catalyze the *cis–trans* conversion of peptidyl-prolyl bonds. Whereas cyclophilins are highly efficient PPIases, PPIase activities

Abbreviations: ER, endoplasmic reticulum; FKBP, FK506-binding proteins; FKBP-EF, FKBP containing the EF-domains; PPIase, peptidyl-prolyl *cis–trans* isomerase.

Grant sponsors: Shriners Hospital for Children (to H.P.B.).

*Correspondence to: Hans Peter Bächinger, Research Department, Shriners Hospital for Children, 3101 SW Sam Jackson Park Road, Portland, OR 97239. E-mail: hpb@shcc.org

of FKBPs are usually moderate, weak or even undetectable. In the noncanonical FKBP members, the FK506-binding site is not conserved and shows neither PPIase activity nor affinity to FK506.[1] A number of FKBP family members contain not only an FK506-binding domain but also possess extra domains such as tetratricopeptide repeat domains, calmodulin binding domains, transmembrane motifs, and others. FKBPs have versatile biochemical functions and are involved in protein folding, receptor signaling, protein trafficking, transcription, apoptosis, and T-cell activation.[1]

FKBPs are found in all living organisms, from bacteria and *archea* to higher plants and mammals, but not in viruses. FKBPs containing EF-hand motifs (FKBP-EFs) are only found in the animal kingdom and present in all species except flatworms, placozoans, and other primitive species (http://supfam.cs.bris.ac.uk/SUPERFAMILY/). The distribution of EF-hand motifs is even wider than that of the FKBP domains, as they are present in all living organisms and even in some viruses. A combination of these two domains in animals is pointing to a specific role of FKBPs containing EF-hand motifs, which should be linked with the appearance of a novel characteristic during evolution.

Two major types of FKBP-EFs should be distinguished, that is, proteins comprising a single FKBP domain and two EF-hand motifs (1FKBP-2EF) and proteins with four FKBP domains and two EF-hand motifs (4FKBP-2EF). It is noteworthy that 4FKBP-2EFs are almost exclusively found in vertebrates, from fishes to mammals, although genes for different FKBP-EF forms with multiple FKBP domains are also found in ascidians. In humans, there are two 1FKBP-2EFs (FKBP22 and 23) and two 4FKBP-2EFs (FKBP60 and 65). All FKBP-EFs have been reported to localize in the endoplasmic reticulum (ER), FKBP22 in *Drosophila*[2] and humans,[3] FKBP23 in mice,[4] and FKBP60 and FKBP65 in mice.[5,6] All FKBP-EFs contain an ER retention signal at the C-terminus. There are two more FKBPs that are localized in the ER, FKBP13 (with one FKBP domain)[7] and potentially FKBP19 (with one FKBP domain and a transmembrane region), but they have no EF-hand motifs. Several EF-hand motif containing proteins have been identified in human ER lumen. The number of EF-hand motifs in these proteins varies from two in multiple coagulation factor deficiency protein 2 (MCFD2) and glucosidase 2 subunit beta to six in proteins of the CREC family, that is, reticulocalbins-1, -2, -3, calumenin, and 45 kDa Ca-binding protein. Among them, MCFD2 structurally resembles the EF-hand portion of FKBP22, as it basically consists of only two EF-hand motifs.[8] MCFD2 interacts in a calcium-dependent manner with LMAN1[9,10] and the MCFD2-LMAN1 complex forms a specific cargo receptor for the ER-to-Golgi transport of coagulation factors V and VIII.[11–13] Interestingly, the MCFD2 interaction with LMAN1 has been shown to be independent from binding to factor VIII,[12] which emphasizes the simultaneous potency of the two-EF-hand-motif structure to form a bridge complex. It is thus possible that the EF-hand motifs of FKBP22 can form complexes with other ER proteins. Indeed, it has been shown that murine FKBP23, which has the same domain organization as FKBP22, binds to 78 kDa glucose-regulated protein (also known as GRP78, HSP70, or BiP).[14]

Studies on FKBP-EFs are of great public health relevance, because mutations in *FKBP14* (FKBP22) cause a variant of Ehlers-Danlos syndrome,[3] and mutations in *FKBP10* (FKBP65) lead to *Osteogenesis Imperfecta*, Bruck syndrome, and *Dentinogenesis Imperfecta*.[15–17]

To provide a structural basis for fully understanding the biological roles of ER-resident FKBPs containing the EF-hand motifs, we determined the three-dimensional structure of human full-length FKBP22 to 1.9 Å.

Results

Overall structure

Native and a selenomethionine derivative of FKBP22 were crystallized, under identical conditions, in space group $P2_1$ with two protein chains per asymmetric unit. The structure of each chain comprises two domains, FKBP, which consists of a single FKBP-type fold, and an EF-hand domain containing two EF-hand motifs [Fig. 1(A)]. The FKBP and EF-hand domains of the same chain are well separated and do not demonstrate significant interactions, which would otherwise stabilize their mutual orientation. The FKBP domain structure is stabilized by an intra-chain disulfide bond between C19 and C77. The classical 12-residue loop of each EF-hand motif coordinates a calcium ion. The C-terminal end of chain A, but not B, coordinates an extra calcium ion. The EF-hand domains of two chains form a dimer in an antiparallel manner [Fig. 1(B)]. An additional binding interface is observed between the FKBP domain and the EF-domain of two different chains. The dimeric complex orients two FKBP-domains in a way that their active sites are separated by a cleft and mutually shifted [Fig. 1(B)]. The cleft has sufficient room to accommodate a polypeptide chain in an extended conformation, which would be accessible by both FKBP active sites.

FKBP-type domain

FKBP12, a canonical FKBP, shares 40% identical residues with the FKBP domain of FKBP22. Secondary structure matching superimposition of FKBP22 and FKBP12 (PDB code: 1FKK)[18] using the secondary-structure matching method[19] demonstrates

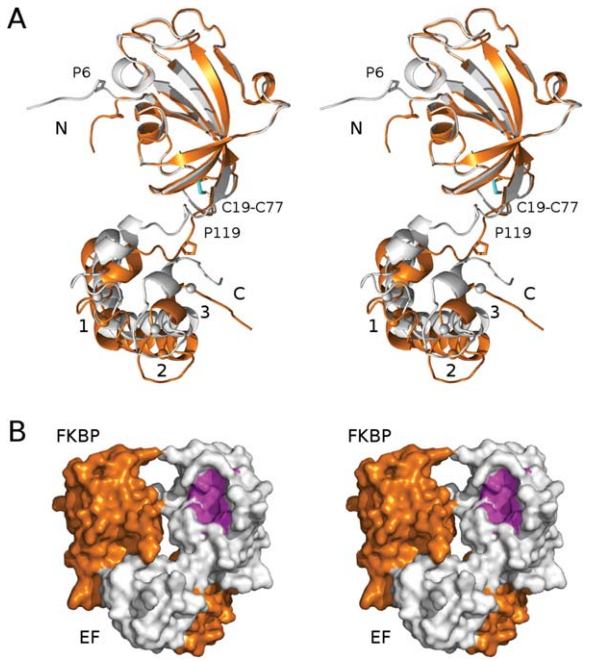

Figure 1. FKBP22 crystal structure. (A) Stereo cartoon topology diagram of FKBP22 A chain (white) and FKBP22 B chain (orange) superimposed using residues 7–116 of the FKBP domain. Calcium ions are shown as spheres and labeled 1, 2, and 3. Disulfide bond C19–C77 is shown in cyan. N- and C-termini are labeled as N and C. (B) Stereo surface diagram of FKBP22 dimer composed of chain A (white) and chain B (orange). The surface of potential PPIases active site of the FKBP domain is shown in magenta. An interactive view is available in the electronic version of the article.

high three-dimensional similarities [residues G1-E107 of FKBP12 and E7-R116 of FKBP22; root mean square deviation (RMSD) of 1.2 and 1.3 Å for 104 equivalent Cα positions for FKBP22 chains A and B, respectively]. Major deviations in the polypeptide backbone between FKBP22 and FKBP12 are mainly observed in regions P16-R21 (an extra residue in FKBP22 and a formation of a disulfide bond between C19 and C77), K39-D40 (an extra K residue), K49-N52 (two extra residues), and G98 (a missing residue). FKBP13, the ER-resident protein with a single FKBP domain, shares 47% sequence identity with the FKBP domain of FKBP22, and the crystal structures are very similar (RMSD 0.9 Å for 100 equivalent Cα positions; human FKBP13 PDB code: 2PBC). It should be noted that the available crystal structure of FKBP13 is N-terminally truncated and neither contains the first β-strand nor the first cysteine which forms a disulfide bond with the second cysteine in homologs. The FKBP domains of chains A and B of the present structure of FKBP22 are structurally identical to each other (RMSD 0.5 Å) and to the structure of the human FKBP22 fragment (RMSD 0.5-0.7 Å, PDB code: 4DIP, chains A–J).

The potential PPIases active site remains largely undisturbed in the FKBP22 molecule. Three out of four residues forming the hydrophobic pocket for the pyrrolidine ring of proline, that is, Y33, W69, and F108 are conserved (Y26, W59, and F99 in FKBP12). The fourth residue, I56 (F46 in FKBP12), provides more room for the ligand and can possibly accommodate modified versions of proline (3- and 4-hydroxyproline). The tyrosine residue (Y92) that coordinates the ligand through hydrogen bonding is also conserved. Nevertheless, of 13 residues of FKBP12 implicated by mutagenesis in binding FK506,[20] only seven are conserved in FKBP22, perhaps reflecting adaptations for a unique substrate specificity.

Interestingly, FKBP22 has an N-terminal tail of sequence ALIPEP that exhibits different orientations in chains A and B of the present structure [Fig. 1(A)] and in the previously published N-terminal fragment of FKBP22 (aka FKBP14; PDB code: 4DIP). The temperature factors for these residues are significantly elevated as well, which indicates higher vibrational motion. Altogether, the N-terminal tail of FKBP22 appears to be highly flexible and can adopt multiple orientations during crystallization, which is suggestive of high disorder in solution. Although it is located near the active site of the FKBP domain, its length is insufficient to reach the active site of either the same or a neighboring chain.

EF-hand domain

The EF-hand domain is formed by two EF-hand motifs. The overall fold is most similar to calcineurin (Z-scores 10.9 and 11.2 for chains A and B by the Dali server[21]). A total of four α-helices are present in the EF-hand domain, together with three loops. Each EF-hand motif contains two α-helices and a classical 12-residue loop structure that coordinates the calcium ion in a pentagonal bipyramidal configuration. Each loop provides a short β-strand (residues 6–10 in the loop numbering) to form an antiparallel β-sheet that stabilizes the structure. Due to the conformational requirements of the backbone, the sixth residue in the loop is most frequently glycine in EF-hand motifs. The second EF-hand motif in FKBP22 contains a glycine (G178), but the first EF-hand motif has a tryptophan (W134). The glycine residue in the second loop of 1FKBP-2EF and 4FKBP-2EF is conserved in all species. Surprisingly, the sixth residue in the first EF-hand loop of 1FKBP-2EF proteins varies in different species: cnidarians—G, D, or K; echinoderms—N or K; nematodes—E; mollusks—N; annelidas—N; arthropods—K; ascidians—K or E; lancelets—K or Q; and vertebrates (W in FKBP22; K or R in FKBP23). The sixth residue in the second EF-hand loop of 4FKBP-2EF proteins (found only in vertebrates) is glycine from amphibians to mammals, but varies in fishes (A, K, R, H, or Q). Presence of a bulkier residue (especially solvent

exposed hydrophobic tryptophan in FKBP22) in the first loop of the EF-hand motif at the position preferentially occupied by the glycine residue in other proteins might reflect involvement of this residue in protein interaction/function.

Analysis of the electron density around the second EF-hand motif of chain A points to a potential extra binding site (secondary, as opposed to the two primary calcium sites in the EF-hand loops) for a metal ion. The ion is coordinated by three oxygen atoms (one from the sidechain carboxyl group of E172 and two from main chain carbonyl groups of E184 and Y187) and by the imidazole sidechain of H189 [Fig. 2(A)]. Although the nature of the ion is inconclusive at the moment, it was modeled with a calcium ion (calcium ions were present in the crystallization solution). The same position in chain B appears to be occupied by a water molecule. It is also coordinated by the carbonyl groups of E184 and Y187 together with an additional water molecule and by the amino group of K188, which would exclude the possibility that this site is another cation [Fig. 2(B)]. The structure of the C-terminal end of chain B (including Y187 and H189) is influenced by the crystal contacts with a symmetrical molecule, whereas the identical region of chain A is free of any crystal contacts. A lower number of coordinating ligands for the additional ion (four instead of seven as in the EF-hand loop) indicate that this site might have a lower affinity/transient interaction. This ion could be involved in the regulation of the protein recycling between the ER and the Golgi as it is adjacent to the ER retention sequence (HDEL) and even coordinated by its histidine side chain. It is interesting to compare sequences of different FKBP-EFs for their potential ability to bind this secondary ion. As residues at positions 184 and 187 coordinate the ion by their main chain carbonyl groups, the nature of their side chains is not directly affecting the binding and thus only the presence of the pair E172–H189 should be considered as an indication for the potential secondary binding site. In vertebrates, this pair of residues is conserved in FKBP22 from fishes to mammals. FKBP23, FKBP60, or FKBP65 do not contain this pair, which makes it a unique feature for FKBP22. Indeed, in all animals starting from primitive ascidians and echinoderms, there is one gene encoding 1FKBP-2EF with the E–H pair, including the only one 1FKBP-2EF found in drosophila.

FKBP-EF interface

The FKBP and EF-hand domains of the same chain are distant and their mutual orientation is not stabilized by interactions between these domains. Indeed, the closest distances between atoms of the domains are between the ϵ-amino group of K24 and the imidazole side chain of H152, 3.0 Å for chain A and 6.6 Å for chain B. The FKBP domains of chains A and B

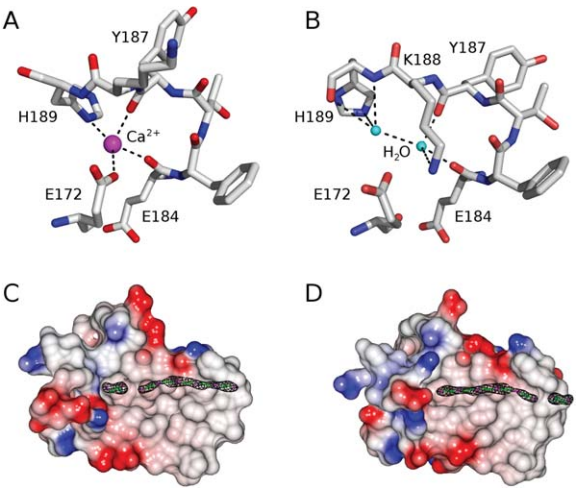

Figure 2. (A) The third calcium ion (magenta) in chain A. (B) The same region in chain B is occupied by two water molecules. (C) Electron density for PEG and 1,2-propanediol molecules calculated using 2Fo-Fc coefficients contoured at 1σ and shown in black on the surface of the EF-hand domain of chain A, which is colored based on electrostatic potential value.[38] (D) The same as in (C) shown for chain B. An interactive view is available in the electronic version of the article.

are structurally identical (RMSD 0.5 Å for Cα positions of residues 7–116) as well as the EF-hand domains (RMSD 0.9 Å for Cα positions of residues 121–186). The two domains are linked by a short linker sequence NGPR (residue numbers 117–120), which demonstrates significant variability of the main chain dihedral angles between chains A and B. Approximating the difference in *pseudo*-dihedral angles[22] of structures A and B as $(\psi_{i,B} + \varphi_{i+1,B}) - (\psi_{i,A} + \varphi_{i+1,A})$, the dihedral rotations are 81°, 26°, 43°, −136°, and 40° for residues 117 through 121, compared with ±<8° for nonhinge residues. From a least-square superimposition of the FKBP domains of chains A and B, significant distance variations are also observed between identical Cα atoms for the linker region (as high as 6.6 Å for prolines 119) and the EF-hand domain (from 2.0 to 6.7 Å).

FKBP22 dimer

The asymmetric unit contains two chains of FKBP22, which form a dimeric complex. The EF-hand domain of each chain forms interactions with both FKBP and EF-hand domains of another chain. No interactions between the FKBP domains of two chains are observed. The dimer has a V-shaped structure, where the EF-hand domains constitute the extended base and the FKBP domains form stalks [Fig. 1(B)]. The potential PPIases active sites of the FKBP domains face the inner space. The cleft between the FKBP domains is sufficient to trace a polypeptide chain in an extended conformation in a way that it can access both catalytic sites. The dimeric interface is established by a set of

Table I. *Molecular Weight of FKBP22 in Solution as Determined by Analytical Ultracentrifugation*

			4°C			20°C
Concentration	20 μM	10 μM	5.0 μM	2.5 μM	1.0 μM	5.0 μM
(wavelength)	(295 nm)	(295 nm)	(280 nm)	(240 nm)	(230 nm)	(280 nm)
Molecular weight	33.2 kDa	29.1 kDa	27.4 kDa	21.7 kDa	23.6 kDa	33.9 kDa

hydrophobic contacts, as well as 19 hydrogen bonds and 15 salt bridges. PISA software[23] shows that the dimer formation buries ~20% of the monomer surface and the solvation free energy gain upon formation of the dimer is −10.7 kcal/mol. The free energy of dimer dissociation has a positive value of 8.4 kcal/mol, which indicates a thermodynamically stable assembly. Based on this free energy, a dissociation constant can be estimated around 1 μM at 37°C. To find out whether FKBP22 forms a dimer in solution, analytical ultracentrifugation studies were performed. Table I summarizes the sedimentation equilibrium data. Recombinant FKBP22 shows a mixed population of monomers and dimers in solution with a shift toward the dimer upon increasing protein concentrations. Strikingly, increased temperature also facilitates the formation of dimers.

Interestingly, the dimeric interface between the two EF-hand domains contains a cavity with prominent electron densities observed in the difference maps (Fo-Fc and 2Fo-Fc). Although nature of the trapped compounds is unknown, we modeled them with one molecule of pentaethylene glycol and one molecule of 1,2-propanediol [Fig. 2(C,D)]. As the recombinant protein was produced in *E.coli*, it remains unclear whether the dimer of FKBP22 in human can trap a specific ligand. The surface of the cavity is rather hydrophobic and can accommodate aliphatic chains. An unknown ligand in the natural form of FKBP22 can potentially facilitate the dimer formation and increase the affinity.

Discussion

The FKBP domain of the ER-resident protein FKBP22 is structurally very similar to the classical FKBP structure of the cytoplasmic protein FKBP12, which has no disulfide bonds. The oxidative environment of the ER allowed the evolution of a form with two cysteines (C19 and C77), which form a disulfide bond and covalently stabilize the FKBP fold. The active site of the FKBP domain is similar to other active FKBPs, so it is reasonable to presume that it is in an active configuration. An enlarged hydrophobic pocket (due to isoleucine substitution of phenylalanine) in the active site can potentially accommodate modified pyrrolidine rings, such as of 3- or 4-hydroxyproline. Surrounding residues of the active site are only partially conserved, which can point to unique substrate specificity. A flexible N-terminal tail near the active site can also be involved in substrate selection/binding as an exosite.

There is an intriguing structural resemblance of the EF-hand domain of FKBP22 with the MCFD2 protein, which mainly consists of two EF-hand motifs and also resides in the ER. The MCFD2 protein forms a complex with LMAN1, and they serve as a specific cargo receptor for coagulation factors V and VIII to transport them from the ER to the Golgi.[11–13] The EF-hand domain of FKBP22 resembles the conformation (RMSD of 1.0 Å) as observed in the MCFD2 complexed with LMAN1.[9,10] Moreover, the area corresponding to the binding interface of MCFD2 to LMAN1 is also accessible in the dimeric form of FKBP22. It is thus possible that FKBP22 might serve as a ligand for transporting yet unknown substrates.

Finding of the potential secondary metal binding site (in addition to the two classical primary sites) at the very C-terminal end of the EF-hand domain seems to be a unique feature for FKBP22. Involvement of the histidine residue from the ER-retention signal (HDEL) in coordination of the ion is intriguing as it can represent a novel calcium mediated mechanism of protein recycling between the Golgi and the ER.

It is unclear whether the dimeric complex observed in the crystal structure of FKBP22 represents a crystallization artifact or a consequence of trapping the unknown compound during expression in *E.coli*. The analytical ultracentrifugation data demonstrate that dimer formation is observed at rather high (and probably non physiological) concentrations. Recombinant production of human FKBP22 in the bacterial system may lack certain factors, which can stabilize dimer formation (e.g., posttranslational modifications and specific ligands). Moreover, dimer formation may possibly be induced/stabilized by a substrate. If the dimerization of FKBP22 is not biologically relevant, then the binding interface is likely to be engaged in interactions with other ER proteins or even with unfolded substrates as it is predominantly formed by hydrophobic side chains. Neveretheless, the dimeric structure of FKBP22 observed in the crystal form somewhat resembles "V-shaped" structures of bacterial FKBPs localized in the periplasmic space.[24,25] They are dimeric molecules divided into two domains. The N-terminal domain includes three helices that are interlaced with those of the other subunit to provide all intersubunit contacts maintaining the dimeric

species. The C-terminal portion is the FKBP domain. The V-shaped structure is important for efficient binding to a protein substrate[26] and crucial for a general chaperone activity.[25] FKBP22 from a filamentous fungus *Nerospora crassa* (not related to animal FKBP22), an ER-resident protein, is also a dimeric protein with PPIase and a chaperone activity, but its homodimerization is mediated by the C-terminal domain (not containing EF-hand motifs) and the N-terminal domain is a functional FKBP domain.[27] The homodimerization is not novel for ER or periplasm resident FKBPs, but the spatial arrangement of FKBP active sites is unique for the structure of human FKBP22, as they are located in close proximity.

Electrophoretic separation of denatured human FKBP22 followed by Western blot analysis revealed a doublet band as indication for a posttranslational modification.[3] One potential modification is glycosylation of N157, which is located between two EF-hand motifs and solvent exposed near the dimer interface. It is thus possible that N157 glysolylation of the endogenous FKBP22 can contribute to stabilization of the dimer.

There is only a single gene encoding FKBP-EF in *Drosophila, Fkbp14*. Recent studies in flies showed that at least partially FKBP22 (aka FKBP14) is likely to function, directly or indirectly, to stabilize presenilin in the ER and that, in the absence of FKBP22, presenilin protein levels are reduced resulting in decreased γ-secretase activity and Notch-related developmental defects.[2] One of the unique features of arthropods is the absence of all types of collagen except type IV, which is a component of the basement membrane. It is possible that FKBP22 can act on different substrates (including multiple collagen types in other animals) and its function is not restricted to the reported one.

Binding of calcium ions by the EF-hand domain of different FKBP-EFs is important for their stability and function. FKBP23 has been shown to bind the GRP78/BiP chaperone in a calcium-dependent manner, potentially playing a role in regulating chaperone activity.[28] Stress-induced changes in ER calcium stores induce the rapid proteolysis of FKBP65, a chaperone and folding mediator of collagen and tropoelastin.[29] Loss of calcium ions in FKBP22 might abolish the dimer formation and any EF-hand domain interactions with other proteins due to loss of the structure. In addition, the FKBP22 recycling in the ER might be affected through the secondary calcium binding site, but further investigations are needed to address this possibility.

Mutations in *FKBP14* (encoding FKBP22) lead to a variant of Ehlers-Danlos syndrome,[3] which is known to be caused by mutations in genes encoding matrix proteins, type III, V, and I collagen, and tenascin-X, as well as enzymes, lysyl hydroxylase-1, ADAMTS2, and β-1,4-galactosyltransferase 7.[30] It remains to be elucidated whether FKBP22 has a direct or indirect effect on folding, trafficking, secretion, or functioning of these proteins or has yet unknown targets.

In summary, the crystal structure of human FKBP22, a prototype of FKBP molecules containing two EF-hand motifs, provides a structural foundation for experimental investigations of the molecular basis several inheritable extracellular matrix disorders, including Ehlers-Danlos syndrome, Bruck syndrome, *Osteogenesis Imperfecta*, and *Dentinogenesis Imperfecta*.

Materials and Methods

Expression and purification of human recombinant FKBP22

DNA encoding human *FKBP14*, without the signal peptide sequence, was amplified from a complementary DNA clone [MGC, ID 4042173 (Invitrogen)] by polymerase chain reaction using primers containing an *EcoRI* site at the 5′ end and a *XhoI* site after the stop codon at the 3′ end. The DNA was cloned into the His-6-tag expression plasmid pET30a(+) (Invitrogen) between the *EcoRI* and *XhoI* restriction sites. The resulting plasmid was transformed into *E. coli* strain BL21 (DE3), cells were grown in a Luria Bertani medium at 37°C to an optical density of 0.6 at 600 nm, the protein expression was induced with 1 m*M* isopropyl β-D-1-thiogalactopyranoside (IPTG) and cells were additionally incubated at 20°C overnight. For the selenomethionine-labeled variant, human FKBP22 was expressed in methionine-deficient *E. coli* strain B834 (DE3) using a medium composed of SelenoMet Medium Base and SelenoMet Nutrient Mix (Athena Enzyme Systems). Cells were harvested by centrifugation and resuspended in B-PER Bacterial Protein Extraction Reagent (Thermo Scientific) containing 1 m*M* $CaCl_2$. Insoluble material was removed by centrifugation and FKBP22 in the soluble fraction was precipitated at 30% (v/v) of saturated ammonium sulfate. After overnight incubation at 4°C the sample was centrifuged and the precipitated material was dissolved in the loading buffer (20 m*M* 4-(2-hydroxyethyl)-1-piperazineethanesulfonic acid (HEPES) buffer, pH 7.5, containing 1.0*M* NaCl, 20 m*M* imidazole, and 1 m*M* $CaCl_2$). The protein solution was filtered through 0.22 μm membrane and applied onto a Co^{2+}-chelating column. After washing with the loading buffer (five column volumes), FKBP22 was eluted with the elution buffer (20 m*M* HEPES buffer, pH 7.5, containing 1.0*M* NaCl, 500 m*M* imidazole, and 1 m*M* $CaCl_2$). The fractions containing FKBP22 were dialyzed against the enterokinase cleavage buffer (50 m*M* Tris/HCl buffer, pH 8.0, containing 1 m*M* $CaCl_2$, and 0.1% Tween 20). Enterokinase (1 unit/mL reaction

Table II. *Summary of Data Collection and Refinement Statistics*

	Se-Met FKBP22	Native FKBP22
Data collection		
Space group	$P2_1$	$P2_1$
a, b, c (Å)	36.6, 100.1, 58.8	36.4, 101.2, 59.0
α, β, γ (°)	90, 99.5, 90	90, 100.0, 90
Resolution[a] (Å)	29.3–2.46 (2.59–2.46)	23.2–1.9 (2.00–1.90)
Measured reflections[a]	52,798 (7,324)	125,712 (18,199)
Unique reflections[a]	15,109 (2,176)	33,131 (4,813)
Redundancy[a]	3.5 (3.4)	3.8 (3.8)
Completeness[a] (%)	99.4 (98.8)	99.8 (99.7)
Matthews coefficient ($Å^3$ Da^{-1})	2.33	2.34
Solvent fraction (%)	47.1	47.5
I/σ (I)[a]	9.3 (2.4)	12.9 (4.2)
Wilson plot B-factor ($Å^2$)	39.8	21.5
R_{merge}[a] (%)	7.7 (43.5)	6.1 (31.5)
Phasing		
PHENIX BAYES-CC/FOM	57.6/0.34	
Refinement		
R-factor (%)		17.3
R_{free} (%)		21.1
Protein/calcium/solvent atoms		3078/5/344
RMSD of bond lengths (Å)		0.006
RMSD of bond angles (°)		1.055
Average B value[b] ($Å^2$)		41.2 (40.8)
Ramachandran favored/ allowed/outliers (%)		98.1/1.6/0.3
MolProbity score[37]		1.46 (96th percentile)

[a] Values in parentheses are for the highest resolution shell.
[b] Values in parentheses are for macromolecule atoms.

volume) (Invitrogen) was used to cleave the His-6-tag at 4°C overnight, and the sample was dialyzed against the loading buffer. To inactivate enterokinase as well as remaining endogenous *E.coli* proteases 1 μL/mL diisopropyl fluorophosphate was added and the solution was gently stirred on ice for 4 h. The sample was then applied onto a Co^{2+}-chelating column to bind the His-6-tag. FKBP22 from the flow through fractions was dialyzed against 20 m*M* triethanolamine/HCl buffer, pH 7.5, containing 20 m*M* NaCl and 0.5*M* urea, loaded onto a HiTrapQ XL column (GE Health Science), and washed with the same buffer (five column volumes). Pure FKBP22 was finally eluted with 30% of 20 m*M* triethanolamine/HCl buffer, pH 7.5, containing 500 m*M* NaCl and 0.5*M* urea.

Crystallization and data collection

The purified human FKBP22 was dialyzed against 1 m*M* Tris/HCl, pH 7.2, containing 0.05 m*M* $CaCl_2$ and concentrated to about 3 mg/mL using the 10-kDa cut-off spin concentrator (Amicon). Both native and selenomethionine-labeled proteins were crystallized at room temperature using the hanging drop vapor diffusion method. For crystallization, 2 μL of the protein solution was mixed with 1 μL of the reservoir solution containing 0.1*M* MES, 25% 1,2-propanediol, and 11–12% polyethylene glycol 20,000, pH 7.0–7.2. The crystals appeared within 1–2 weeks.

Data collection was performed using crystals flash-frozen to 100 K on the "NOIR-1" detector system at the Molecular Biology Consortium Beamline 4.2.2 of the Advanced Light Source, Lawrence Berkeley National Laboratory, Berkeley, California.

Crystal structure determination

The diffraction images were indexed, integrated, and scaled using iMOSFLM[31] and SCALA from the CCP4 suite.[32] Selenomethionine crystals were used for a three-wavelength MAD data collection (Table II) procedure. The program PHENIX[33] was used for the determination of Se atom positions, phasing, density modifications, and automatic building of a partial model (~40%). The map quality was insufficient for robust manual tracing of the remaining parts of two FKBP22 molecules. The AMORE program[34,35] was used within the CCP4 suite[32] to find initial molecular replacement solutions. A crystal structure of the FKBP domain (residues 19–138) of human FKBP22 (aka FKBP14, PDB code: 4DIP) was used as a search model. Two outstanding solutions were generated by AMORE, which corresponded to the FKBP domains in two molecules of FKBP22. Incorporation of the molecular replacement solutions into the asymmetric unit increased the model completeness to ~65%. Iterative cycles of model extension/correction and refinement were performed using the native data set with the aim of programs COOT[36] and PHENIX,[33] respectively. At

the final steps of refinement, three groups of TLS were applied, two for each FKBP domain of chains A and B and one for the EF-hand domain dimer (composed of the two EF-hand domains from the two chains).

Five calcium ions were located in the EF-hand domains. A short fragment of polyethylene glycol and one molecule of 1,2-propanediol were fitted in the extended cavity formed by the EF-hand domains of the two protein molecules. Another short fragment of polyethylene glycol and a number of 1,2-propanediol molecules were also fitted on the surface of FKBP22. The quality of the models was assessed with program MolProbity.[37]

Data collection and refinement statistics are summarized in Table II. Figures were generated with programs PyMOL (http://www.pymol.org) and CCP4MG.[38]

Atomic coordinates

The atomic coordinates and structural factors have been deposited with the Protein Data Bank (PDB code: 4MSP).

Analytical ultracentrifugation

Sedimentation equilibrium measurements were performed with a Beckman model XLA analytical ultracentrifuge. Samples were in Tris buffered saline containing 1 m*M* $CaCl_2$. Runs were carried out at 4 or 20°C in an An60-Ti rotor using 12-mm cells and Epon two-channel centerpieces. The rotor speed used was 20,000 rpm. Data analysis was performed using the Scientist software (MicroMath).

References

1. Kang CB, Hong Y, Dhe-Paganon S, Yoon HS (2008) FKBP family proteins: immunophilins with versatile biological functions. Neurosignals 16:318–325.
2. van de Hoef DL, Bonner JM, Boulianne GL (2013) FKBP14 is an essential gene that regulates Presenilin protein levels and Notch signaling in Drosophila. Development 140:810–819.
3. Baumann M, Giunta C, Krabichler B, Ruschendorf F, Zoppi N, Colombi M, Bittner RE, Quijano-Roy S, Muntoni F, Cirak S, Schreiber G, Zou Y, Hu Y, Romero NB, Carlier RY, Amberger A, Deutschmann A, Straub V, Rohrbach M, Steinmann B, Rostasy K, Karall D, Bonnemann CG, Zschocke J, Fauth C (2012) Mutations in FKBP14 cause a variant of Ehlers-Danlos syndrome with progressive kyphoscoliosis, myopathy, and hearing loss. Am J Hum Genet 90:201–216.
4. Nakamura T, Yabe D, Kanazawa N, Tashiro K, Sasayama S, Honjo T (1998) Molecular cloning, characterization, and chromosomal localization of FKBP23, a novel FK506-binding protein with Ca2+-binding ability. Genomics 54:89–98.
5. Shadidy M, Caubit X, Olsen R, Seternes OM, Moens U, Krauss S (1999) Biochemical analysis of mouse FKBP60, a novel member of the FKPB family. Biochim Biophys Acta 1446:295–307.
6. Patterson CE, Schaub T, Coleman EJ, Davis EC (2000) Developmental regulation of FKBP65. An ER-localized extracellular matrix binding-protein. Mol Biol Cell 11: 3925–3935.
7. Nigam SK, Jin YJ, Jin MJ, Bush KT, Bierer BE, Burakoff SJ (1993) Localization of the FK506-binding protein, FKBP 13, to the lumen of the endoplasmic reticulum. Biochem J 294 (Pt 2):511–515.
8. Guy JE, Wigren E, Svard M, Hard T, Lindqvist Y (2008) New insights into multiple coagulation factor deficiency from the solution structure of human MCFD2. J Mol Biol 381:941–955.
9. Wigren E, Bourhis JM, Kursula I, Guy JE, Lindqvist Y (2010) Crystal structure of the LMAN1-CRD/MCFD2 transport receptor complex provides insight into combined deficiency of factor V and factor VIII. FEBS Lett 584:878–882.
10. Nishio M, Kamiya Y, Mizushima T, Wakatsuki S, Sasakawa H, Yamamoto K, Uchiyama S, Noda M, McKay AR, Fukui K, Hauri HP, Kato K (2010) Structural basis for the cooperative interplay between the two causative gene products of combined factor V and factor VIII deficiency. Proc Natl Acad Sci U S A 107: 4034–4039.
11. Zhang B, Cunningham MA, Nichols WC, Bernat JA, Seligsohn U, Pipe SW, McVey JH, Schulte-Overberg U, de Bosch NB, Ruiz-Saez A, White GC, Tuddenham EG, Kaufman RJ, Ginsburg D (2003) Bleeding due to disruption of a cargo-specific ER-to-Golgi transport complex. Nat Genet 34:220–225.
12. Zhang B, Kaufman RJ, Ginsburg D (2005) LMAN1 and MCFD2 form a cargo receptor complex and interact with coagulation factor VIII in the early secretory pathway. J Biol Chem 280:25881–25886.
13. Nyfeler B, Zhang B, Ginsburg D, Kaufman RJ, Hauri HP (2006) Cargo selectivity of the ERGIC-53/MCFD2 transport receptor complex. Traffic 7:1473–1481.
14. Zhang X, Wang Y, Li H, Zhang W, Wu D, Mi H (2004) The mouse FKBP23 binds to BiP in ER and the binding of C-terminal domain is interrelated with Ca2+ concentration. FEBS Lett 559:57–60.
15. Alanay Y, Avaygan H, Camacho N, Utine GE, Boduroglu K, Aktas D, Alikasifoglu M, Tuncbilek E, Orhan D, Bakar FT, Zabel B, Superti-Furga A, Bruckner-Tuderman L, Curry CJ, Pyott S, Byers PH, Eyre DR, Baldridge D, Lee B, Merrill AE, Davis EC, Cohn DH, Akarsu N, Krakow D (2010) Mutations in the gene encoding the RER protein FKBP65 cause autosomal-recessive osteogenesis imperfecta. Am J Hum Genet 86:551–559.
16. Steinlein OK, Aichinger E, Trucks H, Sander T (2011) Mutations in FKBP10 can cause a severe form of isolated Osteogenesis imperfecta. BMC Med Genet 12:152.
17. Kelley BP, Malfait F, Bonafe L, Baldridge D, Homan E, Symoens S, Willaert A, Elcioglu N, Van Maldergem L, Verellen-Dumoulin C, Gillerot Y, Napierala D, Krakow D, Beighton P, Superti-Furga A, De Paepe A, Lee B (2011) Mutations in FKBP10 cause recessive osteogenesis imperfecta and Bruck syndrome. J Bone Miner Res 26:666–672.
18. Wilson KP, Yamashita MM, Sintchak MD, Rotstein SH, Murcko MA, Boger J, Thomson JA, Fitzgibbon MJ, Black JR, Navia MA (1995) Comparative X-ray structures of the major binding protein for the immunosuppressant FK506 (tacrolimus) in unliganded form and in complex with FK506 and rapamycin. Acta Crystallogr D Biol Crystallogr 51:511–521.
19. Krissinel E, Henrick K (2004) Secondary-structure matching (SSM), a new tool for fast protein structure

alignment in three dimensions. Acta Crystallogr D Biol Crystallogr 60:2256–2268.
20. DeCenzo MT, Park ST, Jarrett BP, Aldape RA, Futer O, Murcko MA, Livingston DJ (1996) FK506-binding protein mutational analysis: defining the active-site residue contributions to catalysis and the stability of ligand complexes. Protein Eng 9:173–180.
21. Holm L, Rosenstrom P (2010) Dali server: conservation mapping in 3D. Nucleic Acids Res 38:W545–549.
22. Levitt M (1976) A simplified representation of protein conformations for rapid simulation of protein folding. J Mol Biol 104:59–107.
23. Krissinel E, Henrick K (2007) Inference of macromolecular assemblies from crystalline state. J Mol Biol 372: 774–797.
24. Riboldi-Tunnicliffe A, Konig B, Jessen S, Weiss MS, Rahfeld J, Hacker J, Fischer G, Hilgenfeld R (2001) Crystal structure of Mip, a prolylisomerase from Legionella pneumophila. Nat Struct Biol 8:779–783.
25. Saul FA, Arie JP, Vulliez-le Normand B, Kahn R, Betton JM, Bentley GA (2004) Structural and functional studies of FkpA from Escherichia coli, a cis/trans peptidyl-prolyl isomerase with chaperone activity. J Mol Biol 335:595–608.
26. Budiman C, Bando K, Angkawidjaja C, Koga Y, Takano K, Kanaya S (2009) Engineering of monomeric FK506-binding protein 22 with peptidyl prolyl cis-trans isomerase. Importance of a V-shaped dimeric structure for binding to protein substrate. FEBS J 276:4091–4101.
27. Tremmel D, Tropschug M (2007) Neurospora crassa FKBP22 is a novel ER chaperone and functionally cooperates with BiP. J Mol Biol 369:55–68.
28. Wang Y, Han R, Wu D, Li J, Chen C, Ma H, Mi H (2007) The binding of FKBP23 to BiP modulates BiP's ATPase activity with its PPIase activity. Biochem Biophys Res Commun 354:315–320.
29. Murphy LA, Ramirez EA, Trinh VT, Herman AM, Anderson VC, Brewster JL (2011) Endoplasmic reticulum stress or mutation of an EF-hand Ca(2+)-binding domain directs the FKBP65 rotamase to an ERAD-based proteolysis. Cell Stress Chaperones 16:607–619.
30. Byers PH, Murray ML (2013) Ehlers-Danlos syndrome: a showcase of conditions that lead to understanding matrix biology. Matrix Biol. pii: S0945-053X(13)00098-X. doi: 10.1016/j.matbio.2013.07.005.
31. Battye TG, Kontogiannis L, Johnson O, Powell HR, Leslie AG (2011) iMOSFLM: a new graphical interface for diffraction-image processing with MOSFLM. Acta Crystallogr D Biol Crystallogr 67:271–281.
32. Collaborative Computational Project N (1994) The CCP4 suite: programs for protein crystallography. Acta Crystallogr D Biol Crystallogr 50:760–763.
33. Adams PD, Afonine PV, Bunkoczi G, Chen VB, Davis IW, Echols N, Headd JJ, Hung LW, Kapral GJ, Grosse-Kunstleve RW, McCoy AJ, Moriarty NW, Oeffner R, Read RJ, Richardson DC, Richardson JS, Terwilliger TC, Zwart PH (2010) PHENIX: a comprehensive Python-based system for macromolecular structure solution. Acta Crystallogr D Biol Crystallogr 66:213–221.
34. Navaza J (2001) Implementation of molecular replacement in AMoRe. Acta Crystallogr D Biol Crystallogr 57:1367–1372.
35. Trapani S, Navaza J (2008) AMoRe: classical and modern. Acta Crystallogr D Biol Crystallogr 64:11–16.
36. Emsley P, Lohkamp B, Scott WG, Cowtan K (2010) Features and development of Coot. Acta Crystallogr D Biol Crystallogr 66:486–501.
37. Chen VB, Arendall WB, 3rd, Headd JJ, Keedy DA, Immormino RM, Kapral GJ, Murray LW, Richardson JS, Richardson DC (2010) MolProbity: all-atom structure validation for macromolecular crystallography. Acta Crystallogr D Biol Crystallogr 66:12–21.
38. McNicholas S, Potterton E, Wilson KS, Noble ME (2011) Presenting your structures: the CCP4mg molecular-graphics software. Acta Crystallogr D Biol Crystallogr 67:386–394.